Journal of Structural Geology, Vol. 15, No. 6, pp. 753 to 770, 1993
Printed in Great Britain

0191-8141/93 $06.00+0.00

Fault and bed 'rotation' during continental extension: block rotation or vertical shear?

ROB WESTAWAY

Department of Geological Sciences, University of Durham, Durham DH1 3LE, U.K.

and

NICK KUSZNIR

Department of Earth Sciences, University of Liverpool, Liverpool L69 3BX, U.K.

(*Received* 13 *February* 1992; *accepted in revised form* 11 *August* 1992)

Abstract—For almost a century, the view has existed that the tilting of blocks between closely-spaced planar normal faults is rigid-body rotation. This interpretation requires only simple geometry, and has consequently found widespread application. However, it is not consistent with the deformation expected around normal faults given the present knowledge of stress fields and rheology in basement in the brittle upper crust, which is better regarded instead as distributed vertical simple shear. Rigid-body rotation and vertical shear involve different relations between fault and bed tilting, and thus predict different initial fault dips for particular present-day dips of faults and beds. These two schemes also predict different amounts of extension, and it is consequently important to establish which is correct. With this aim in mind, we examine normal faults associated with Neogene extension in western Turkey and the western United States, and with Mesozoic extension in the North Sea. Except where extension and the associated tilting are minimal, rigid-body rotation predicts unrealistically steep initial fault dips. Some extensional basins also exhibit reversals of normal fault polarity and tilt polarity of beds, which are incompatible with rigid-body rotation. We therefore conclude that the general cause of the tilting is vertical shear, not rigid-body rotation. This has three main observational consequences. First, the heave on any normal fault equals the amount of extension across it. Second, no feature near a normal fault can rotate through the vertical. A normal fault thus cannot rotate through the vertical and appear as a reverse fault. Third, any initially-vertical feature near a normal fault will remain vertical. A vertical dyke in the tilted surroundings of a normal fault is thus not necessarily younger than the extension that caused the tilting.

INTRODUCTION

DURING continental extension, the upper mantle and lower crust appear to extend plastically, principally by distributed pure shear. In contrast, the upper crust, shallower than ~15 km depth, is brittle, and extends by slip on normal faults. These faults appear to be planar rather than listric within basement in the upper crust, on the basis of seismic reflection observations (e.g. Roberts & Yielding 1991), earthquake studies (e.g. Jackson 1987) and geodetic analyses (e.g. Stein & Barrientos 1985). As a consequence of slip on any such normal fault, older stratigraphy becomes tilted. Beds within this stratigraphy (or other surfaces that are initially horizontal, such as unconformities or erosion surfaces) act as convenient passive markers to determine the extent of this tilting. It is inferred that the faults that control the extension of the upper crust also tilt, developing progressively less steep dips as extension proceeds. A typical cross-section through extended upper crust showing major planar normal faults in basement and tilted bedding, for Mesozoic extension of the northern North Sea, is shown in Fig. 1.

Many people (e.g. Emmons & Garrey 1910, Morton & Black 1975, Jackson & McKenzie 1983, Jackson 1987) have noted that normal faults are often closely-spaced, with blocks between them narrow compared with their vertical extent. In localities where the major normal faults that control extension have the same polarity and approximately equal spacing, the resulting quasi-periodic tilting of beds and the inferred tilting of closely-spaced faults gives the impression that the fault-

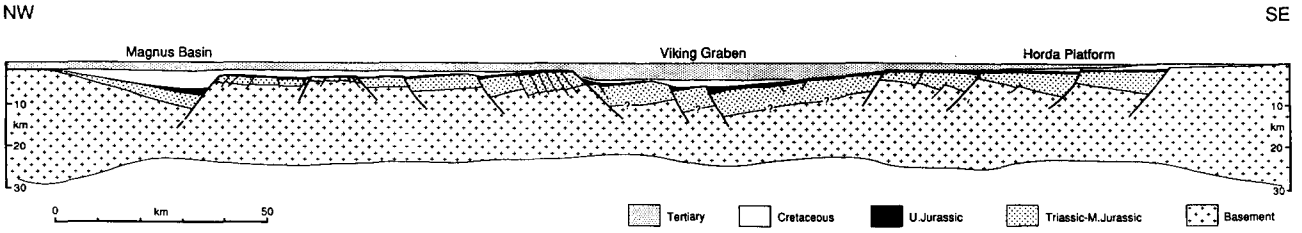

Fig. 1. Cross-section across the Viking graben in the northern North Sea, showing Mesozoic normal faults with irregular spacings and polarity reversals, with tilting substantial in basement near major normal faults but dying out towards the edges of the extensional province. Adapted from fig. 2 of Marsden *et al.* (1990).

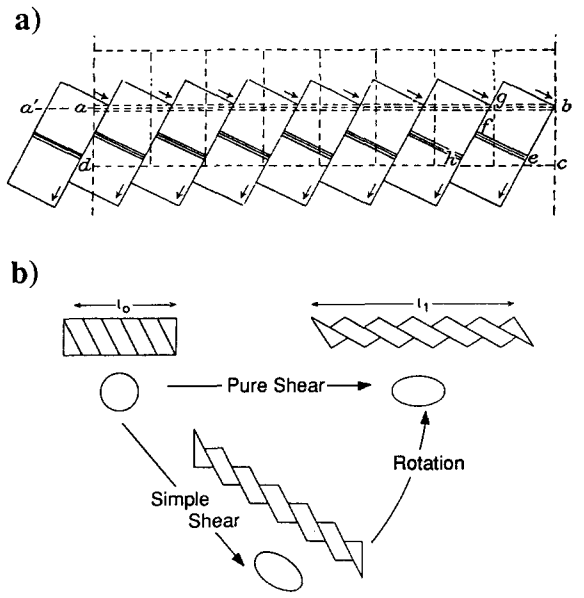

Fig. 2. Schematic cross-sections showing extension accompanied by rigid-body rotation. (a) The proportionality between fault spacing and displacement that is required to maintain constant rotation. This historic diagram, adapted from fig. 15 of Emmons & Garrey (1910) was—to the best of our knowledge—the first ever portrayal of 'rigid domino' extension. (b) Representation after Jackson's (1987 fig. 4) model that extensional pure shear can be partitioned as simple shear localized on normal faults and rigid-body rotation. Extension factor β equals L_1/L_0.

bounded blocks have rotated around horizontal axes. Such blocks have been likened to dominoes, and it has been suggested that they are infinitely rigid and take up extension by rigid-body rotation (e.g. Jackson 1987) (Fig. 2).

For rigid-body rotation, tilt angles of beds and faults are identical. This assumption is frequently used to determine initial dips of normal faults (e.g. Jackson 1987). Let θ denote the present-day dip of a surface that was horizontal when extension began. If the initial and present-day fault dips are δ_0 and δ (with fault tilt $\psi = \delta_0 - \delta$), then for rigid-body rotation:

$$\theta = \delta_0 - \delta = \psi. \quad (1)$$

For example, if the steepest beds in a basin dip at 15°, and the normal fault at its margin dips at 45°, with this assumption one may deduce an initial fault dip of 60°. An angle $\varkappa$ can be defined as the difference of tilt between a normal fault and a surface in its surroundings that was horizontal when extension began:

$$\varkappa = \theta - \psi. \quad (2)$$

For rigid-body rotation $\varkappa$ is thus always zero. We suggest the name 'tilt discrepancy' for $\varkappa$.

For coseismic processes, the vertical partitioning and distribution of vertical displacements between the hanging-wall and footwall of a normal fault can be modelled using elastic dislocation theory within a self-gravitating lithosphere (e.g. Stein & Barrientos 1985, King *et al.* 1988), which can be well-approximated as an elastic halfspace because the vertical extent of faulting (~15 km) is much less than the typical lithosphere thickness (~100 km) (Fig. 1). On longer time scales (perhaps on interseismic time scales of thousands of years, perhaps over ~100,000 years), viscoelastic relaxation within the lower crust and mantle lithosphere redistributes the vertical forces generated by extension. As a consequence of time-dependent creep in the lower crust and mantle lithosphere, the response of the lithosphere changes over these time scales from that of a self-gravitating elastic halfspace containing a finite cut to that of a self-gravitating brittle–elastic upper-crustal plate above a fluid substratum. The final distribution of vertical displacements within the hanging-wall and footwall of a normal fault in basement is thus the sum of many coseismic displacements plus the cumulative postseismic viscoelastic relaxation (e.g. King *et al.* 1988).

The viscoelastic redistribution of the isostatic forces generated by extension does not appear to be associated with additional upper-crustal extension or slip on major faults, or with other significant seismic activity. Its principal observable consequence is uplift throughout each normal fault zone, which adds to the coseismic footwall uplift and cancels part of the coseismic hanging-wall subsidence (e.g. King *et al.* 1988). The absolute coseismic hanging-wall subsidence is typically 5–10 times the absolute footwall uplift (e.g. Stein & Barrientos 1985, King *et al.* 1988). In contrast, after relaxation absolute coseismic hanging-wall subsidence and footwall uplift are more equal, with their precise ratio dependent on the amounts of hanging-wall loading and footwall erosion (e.g. King *et al.* 1988, Kusznir *et al.* 1991). The long-term viscoelastic redistribution of isostatic forces thus appears to be accommodated by mainly vertical displacements in response to the bending of a thin, self-gravitating, upper-crustal plate. Neither coseismically nor post-seismically do footwalls and hanging-walls of normal faults appear to behave as infinitely rigid blocks undergoing rigid-body rotation. Laterally varying distributed vertical simple shear appears instead to be a more appropriate way to describe their postseismic response and the resulting cumulative deformation.

Other fundamental problems of rigid-body rotation (Fig. 2) are its failure to explain how normal-fault polarities can switch within extensional regions, or how these regions terminate laterally (Fig. 3). Nor does it permit arbitrary spacing or displacement on adjacent faults; spacing and displacement must be in proportion to maintain constant rotation (Fig. 2a). It is difficult to see how these aspects of the behaviour of real normal-fault systems (e.g. Fig. 1) can occur without internal deformation of fault-bounded blocks.

UPPER-CRUSTAL VERTICAL SHEAR DURING EXTENSION

Buck (1988) and Kusznir *et al.* (1991) have shown that the elastic bending stress associated with flexure and the development of curvature within the brittle layer around an isolated planar normal fault is large, and will cause

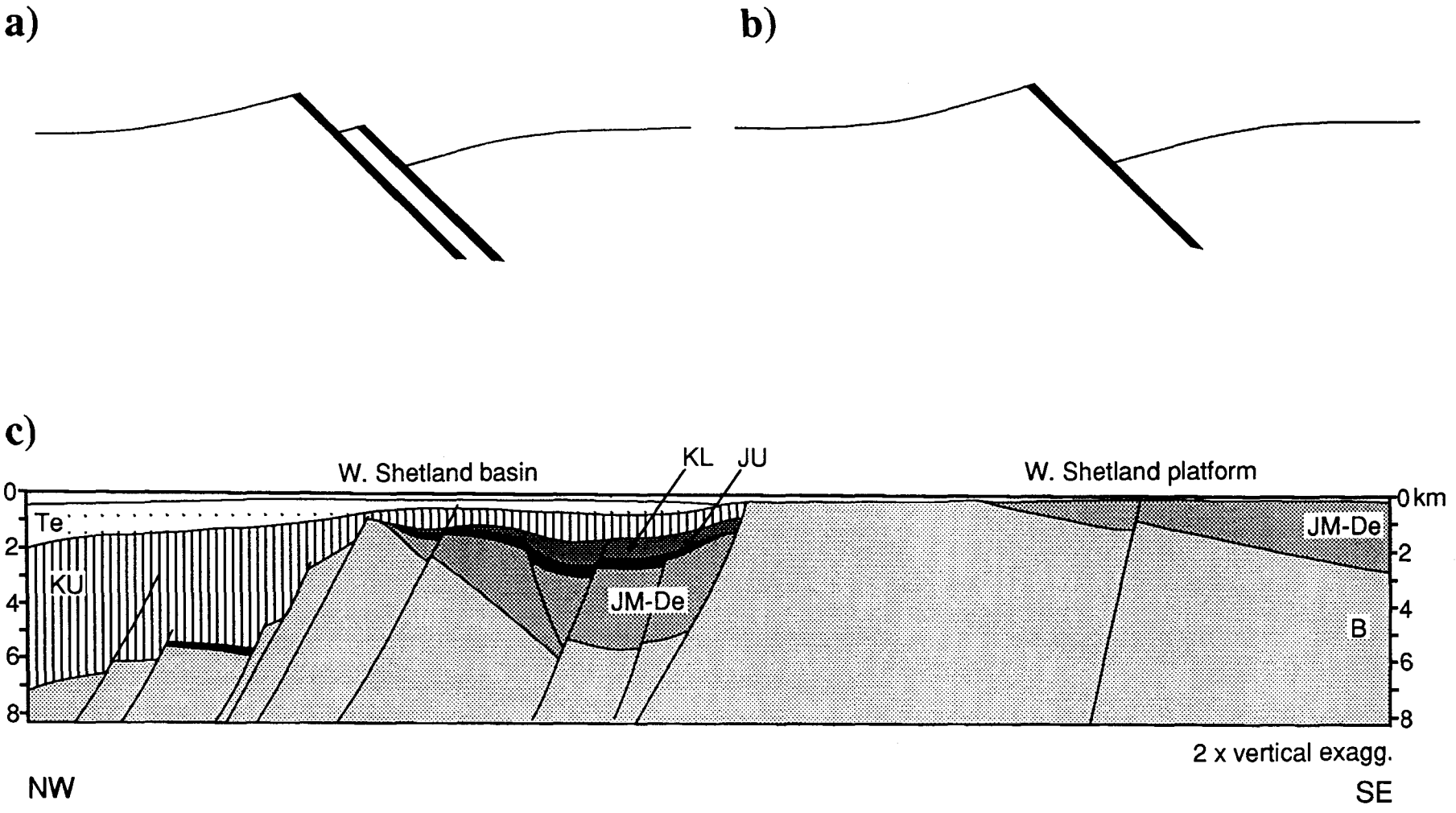

Fig. 3. (a) & (b) Schematic diagram of an isolated normal fault zone that (a) does and (b) does not contain subparallel closely-spaced en échelon branches. One would expect the same deformation style in both cases, because overall they differ minimally. In (a), one would traditionally regard the block between these branches as a rigid 'domino'. If so, δ and θ for both this block and its immediate surroundings outside the fault zone would satisfy equation (1). One would expect the same to be true for (b) also. Likewise, both (a) and (b) can be interpreted instead assuming vertical shear, in which case δ and θ are expected to satisfy equation (6). (c) Cross-section across the West Shetland basin (to the west of the Shetland Islands, offshore of northern Scotland), adapted from fig. 48 of Ziegler (1988). Te, Tertiary sediment; KU, Upper Cretaceous; KL, Lower Cretaceous; JU, Upper Jurassic; JM-De, Middle Jurassic to Devonian; B, Pre-Devonian basement. The closely-spaced normal faults beneath the West Shetland basin dip NW at 43°; top basement dips SE at 22°. Is the observed tilting of *these* faults and blocks by vertical shear or by rigid-body rotation?

brittle failure in the surroundings of the fault if realistic mechanical properties are assumed. As a result, the rigidity of the blocks bounding any isolated normal fault cannot reasonably be regarded as infinite, and may indeed be quite small, corresponding to an effective elastic thickness of only a few kilometres. This reasoning against an infinite rigidity for normal-fault-bounded blocks also applies for systems of multiple faults.

Jackson (1987) proposed a scheme for extension of the brittle layer where extensional pure shear is achieved by partitioning deformation into rigid-body rotation of blocks around horizontal axes and simple shear, the simple shear being parallel to and localized on each fault plane (Fig. 2b). On a regional scale, over many normal faults, the brittle layer can take up deformation that is equivalent to extensional pure shear. However, on the scale of an individual normal fault a more realistic way to partition deformation treats the horizontal displacement perpendicular to fault strike, the heave, as taking up extension by enabling blocks to separate (Fig. 4), whereas its vertical component, the throw, enables each fault to accommodate local tilting, which results from the need to maintain isostatic equilibrium as the footwall becomes unloaded and the hanging-wall becomes loaded during extension. Most recent schemes for normal faulting, whether qualitative (e.g. Wernicke & Axen 1988) or quantitative (e.g. Buck 1988, Kusznir *et al.* 1991), incorporate distributed vertical simple shear

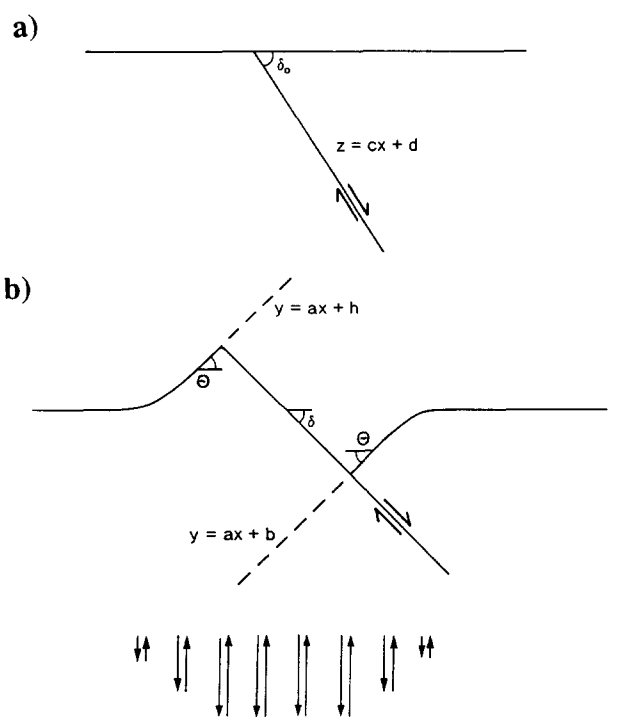

Fig. 4. Schematic summary of tilting around an isolated normal fault by distributed vertical simple shear. In (a) the fault forms with initial dip δ_o. In (b), after some extension, the fault has dip δ and a surface that was initially horizontal now has dip θ adjacent to it. As is shown in the text, angles δ_o, δ and θ are related by equation (6). Paired vertical arrows beneath (b) indicate the sense and relative magnitude of vertical simple shear strain at different horizontal positions along the tilted surface and in the vicinity of the fault plane. On the scale that we consider, we regard this vertical shear as distributed; not, for example, localized on vertical faults.

to some extent. With vertical shear occurring in both the footwall and hanging-wall of a normal fault, the heave on the fault will equal the amount of extension across it. Moving away from an isolated fault, one would expect the vertical simple shear strain to decrease to zero, as in Fig 4(b). Between closely-spaced subparallel normal faults, this strain would not be expected to vary substantially, causing roughly uniform tilting. Uniform tilting of blocks between closely-spaced normal faults is thus not necessarily caused by rigid-body rotation: it may arise instead through uniform vertical shear.

Many people have developed flexural solutions for deformation in the surroundings of normal faults (e.g. Buck 1988, Kusznir *et al.* 1991). Flexure differs in principle from ideal vertical shear, insofar as it involves blocks laterally dilating and/or contracting above and below a neutral fibre whose length is unchanged. However, where curvature of the surroundings to a normal fault is gentle, with radius of curvature large compared with the horizontal extent of tilting, the deflection predicted for flexure will be subvertical, such that it approximates vertical shear. Thin plate flexure theory neglects horizontal displacements, and methods based on it (e.g. Kusznir *et al.* 1991) thus predict displacements that are equivalent to vertical shear. Wernicke & Axen (1988) suggested instead that *footwall* uplift is by ideal vertical shear, although hanging-wall subsidence is not.

Each of the above schemes (Buck 1988, Wernicke & Axen 1988, Kusznir *et al.* 1991) predicts deformation of basement in the surroundings to normal faults. Their assumption that the vertical simple shear strain is uniform in each vertical column in the brittle layer means that it is different at different depths adjacent to the fault. This means that, as extension proceeds, a normal fault that is initially planar will gradually cease to be precisely planar, because different parts of it will be in localities with different vertical simple shear strain. The inferred bending of fault planes is assumed to occur on the post-seismic time scale.

Compared with Wernicke & Axen (1988), some other schemes for deformation around normal faults assume even greater differences between hanging-wall and footwall deformation styles, requiring footwalls to remain fixed as hanging-walls tilt. In these schemes, decreases in hanging-wall tilting away from any normal fault require the fault to be listric. Verrall (1981) proposed a geometrical method for investigating *hanging-wall* tilting, which assumes that it accompanies distributed vertical simple shear. White *et al.* (1986) developed this method to cover inclined distributed hanging-wall simple shear, suggesting that this shear is typically oriented at ~45° in the antithetic sense. These two schemes assume and require fundamentally different rheology and deformation mechanisms for hanging-walls and footwalls. This assumption makes no sense when dealing with deformation in basement that is the same on both sides of a fault. Neither scheme incorporates the isostatic response to displacement on a normal fault. Furthermore, it is evident from many of our figures that normal fault footwalls have tilted. For these reasons we exclude

schemes that require fixed footwalls. It is noteworthy that many localities formerly interpreted using Verrall's (1981) method are now regarded as having taken up extension accompanied by both footwall and hanging-wall tilting instead (e.g. Roberts & Yielding 1991).

While major normal faults in basement, which take up coseismic extension, are approximately planar (e.g. Jackson 1987), the elastic dislocation theory that governs coseismic deformation does not require precisely planar shape. Minor fault curvature and changes in fault dip are entirely reasonable. Westaway *et al.* (1989) documented a normal fault in basement in Italy with 60° dip at the Earth's surface and 48° dip at ~10 km depth, indicating average fault curvature of $\sim 0.03\ km^{-1}$. This is within the range of surface curvature observed near basement-bounding normal faults and attributable to elastic flexure (see, e.g., Kusznir *et al.* 1991), and is presumably accommodated by the wall rocks to the fault flexing. Curvatures of this order correspond to bending stresses that approach the limit for crustal rock, and thus require some brittle failure (see, e.g., Kusznir *et al.* 1991). Much sharper fault curvature has of course been documented by many people in weak materials, such as unconsolidated sediments. In the absence of well-documented sharp curvature on normal faults in basement, we believe it is reasonable to assume that these faults typically initiate planar and remain approximately planar as they take up extension. We suggest that this may be because the initial elastic strength of the basement enables it to resist the development of sharp fault curvature. Alternatively, if moderate fault curvature were to develop, the resulting stress may well be sufficient to shear off the block on the concave side of the fault, restoring it to approximately planar geometry. Conversely, if for some reason sharp curvature of a normal fault in basement were to develop, more complex deformation would probably be required in its surroundings.

The above arguments suggest that bed and block tilting occur by a combination of coseismic elastic dislocation response and post-seismic vertical shear to restore isostatic equilibrium, rather than by rigid-body rotation, and can be regarded overall as vertical shear, to a good approximation at least. This deformation style imposes no constraints on fault displacements, orientations and spacings. It thus permits normal fault systems to exist with irregular displacements, orientations and spacings—behaviour that is incompatible with the rigid domino model. In the next section it is also shown that the relationships between tilts of beds and faults for vertical shear also differ fundamentally from those for rigid-body rotation.

'ROTATION' OF FAULTS AND BEDS BY VERTICAL SHEAR

We now pursue quantitatively some consequences of the assumption of ideal distributed vertical simple shear in the surroundings to normal faults, to derive the relationship between the tilting of normal faults and dip of the oldest beds adjacent to them. Consider the geometrical configuration in Fig. 4, where a planar normal fault has initial dip δ_o, where $\tan(\delta_o) = -c$, and satisfies the equation:

$$z = cx + d. \tag{3}$$

A general scheme for ideal distributed vertical simple shear will cause lateral variations in fault and bed tilting as a result of lateral variations in vertical shear. Let us consider the relationship between fault and bed tilting by ideal vertical shear in the limit of infinitesimal distance from the fault. In this limit, the fault can be assumed locally planar, with local dip δ.

Suppose extension is accompanied by ideal distributed vertical simple shear that acts to tilt an initially horizontal marker (such as a bed that was deposited at the start of extension, or an older bed or other surface that was subhorizontal at that time) by angle θ, where $\tan(\theta) = a$, and also acts to tilt the fault. Suppose that after extension this initially-horizontal marker locally has equation:

$$y = ax + b. \tag{4}$$

Adjacent points on the fault will now have vertical co-ordinate $v(x)$, where $v = z + y$. Thus:

$$\begin{aligned} v = z + y &= cx + d + ax + b \\ &= (c + a)x + (b + d). \end{aligned} \tag{5}$$

As a result of this vertical shear, the fault dip δ will be such that $\tan(\delta) = -(c + a)$.
Substituting for c and a gives:

$$\tan(\delta) = \tan(\delta_o) - \tan(\theta)$$

or

$$\tan(\theta) = \tan(\delta_o) - \tan(\delta) \tag{6}$$

which can be compared with equation (1) that assumes rigid-body rotation. Following equation (6), if beds dip at 15° near a normal fault with dip 45°, one should deduce that the fault had initial dip 52°, not 60° as before. The assumed distributed vertical simple shear has the same sense (in this case, down-to-the-left) on both sides of the fault in Fig. 4(b). Because this fault is drawn planar, in this case this shear strain is the same adjacent to it on both sides, equal to a or $\tan(\theta)$, and gradually decreases to zero away from this fault on both sides.

Recalling that fault tilt ψ equals $\delta_o - \delta$, then $\delta = \delta_o - \psi$, and given the general trigonometrical relationship that:

$$\tan(\delta_o - \psi) \equiv \frac{\tan(\delta_o) - \tan(\psi)}{1 + \tan(\delta_o)\tan(\psi)} \tag{7}$$

equation (6) can be written in terms of ψ as:

$$\tan(\delta) = \tan(\delta_o) - \tan(\theta) = \frac{\tan(\delta_o) - \tan(\psi)}{1 + \tan(\delta_o)\tan(\psi)} \tag{8}$$

or

$$\tan(\theta) = \frac{[\tan(\psi)\tan^2(\delta_o)]}{1 + \tan(\delta_o)\tan(\psi)}. \quad (9)$$

Equation (9) can then be rewritten as:

$$\tan(\theta) = f\tan(\psi) \quad (10)$$

to give the relationship between bed and fault tilt, where

$$f = \frac{1 + \tan^2(\delta_o)}{1 + \tan(\delta_o)\tan(\psi)}. \quad (11)$$

As one moves away from any isolated normal fault the dip of any bed will decrease, eventually becoming zero. These equations cover dips of beds when immediately adjacent to faults, and to apply them thus requires bed dip measurements in suitable localities immediately adjacent to faults. The distance over which bed dip decreases depends on the effective elastic thickness of the upper crust (e.g. King *et al.* 1988, Kusznir *et al.* 1991) and is not quantifiable simply in terms of geometry. Because any curved normal fault can be approximated as the limit of a large number of small planar patches, these equations will apply to tilting adjacent to each patch taken separately, provided this tilting comprises distributed vertical simple shear. However, as already noted, deformation near any strongly-curved normal fault in basement would be expected to be more complex than distributed vertical simple shear, and we expect the useful application of these equations to be limited mainly to normal faults that are planar or approximately planar.

The upper limit for ψ is δ_o, which occurs when a normal fault has tilted to horizontal orientation (Table 1). However, in some cases when normal faults tilt sufficiently that their dips approach ~30°, a new generation of fault may form nearby to take up continuing extension (Jackson & McKenzie 1983, Jackson 1987). If so, this limit is never reached. From equation (11) a necessary condition for $f > 1$, which gives $\theta > \psi$ and $\varkappa > 0°$, is that $\psi < \delta_o$. Given that $\psi = \delta_o - \delta$, this condition is equivalent to $\delta > 0°$. Thus, for *all* non-zero dips of normal faults, vertical shear makes bed tilt exceed fault tilt, with $\varkappa > 0°$. Depending on δ_o, $\varkappa$ can indeed sometimes be substantial (Table 1).

Although $\varkappa$ is positive for all non-zero dips of normal faults and all positive values of ψ, it does not increase monotonically with increasing ψ or decreasing δ (Table 1). Values of $\varkappa$ decrease at large ψ, reaching zero when $\psi = \delta_o$. For a fault in this regime, increments to bed tilt will be smaller than the corresponding increments to fault tilt. The relationship between $\varkappa$ and ψ is thus significant. It can be obtained by substituting $\psi = \delta_o - \delta$ and $\theta = \varkappa + \psi$ into equation (6), expanding the resulting equation using multiple-angle formulae equivalent to equation (7), and rearranging:

$$\tan(\varkappa) = \frac{\tan^2(\delta_o)\tan(\psi) - \tan(\delta_o)\tan^2\psi}{1 + \tan(\delta_o)\tan(\psi) + \tan^2(\delta_o)\tan^2(\psi) + \tan^2(\psi)}. \quad (12)$$

Table 1. Normal fault and bed tilting assuming distributed vertical simple shear

Fault tilt($\psi = \delta_o - \delta$)	Bed tilt (θ)	$\varkappa = (\theta - \psi)$
	$\delta_o = 0°$	
0.0	0.0	0.0
>0.0	impossible	
	$\delta_o = 15°$	
0.0	0.0	0.0
7.4	7.6	0.26148
7.5	7.8	0.26140
15.0	15.0	0.0
>15.0	impossible	
	$\delta_o = 30°$	
0.0	0.0	0.0
7.5	9.3	1.8
13.9	16.1	2.20
15.0	17.2	2.19
22.5	24.0	1.5
30.0	30.0	0.0
>30.0	impossible	
	$\delta_o = 45°$	
0.0	0.0	0.0
7.5	13.1	5.6
15.0	22.9	7.9
18.4	26.6	8.1
22.5	30.4	7.9
30.0	36.2	6.2
37.5	41.0	3.5
45.0	45.0	0.0
>45.0	impossible	
	$\delta_o = 60°$	
0.0	0.0	0.0
7.5	23.2	15.7
15.0	36.2	21.2
19.1	40.9	21.8
22.5	44.0	21.5
30.0	49.1	19.1
37.5	52.8	15.3
45.0	55.7	10.7
52.5	58.0	5.5
60.0	60.0	0.0
>60.0	impossible	
	$\delta_o = 75°$	
0.0	0.0	0.0
7.5	52.8	45.3
13.2	61.8	48.6
15.0	63.4	48.4
22.5	67.6	45.1
30.0	69.9	39.9
37.5	71.4	33.9
45.0	72.4	27.4
52.5	73.2	20.7
60.0	73.9	13.9
67.5	74.5	7.0
75.0	75.0	0.0
>75.0	impossible	

See text for discussion

This equation can be simplified by substituting $D = \tan(\delta_o)$, $P = \tan(\psi)$, and $K = \tan(\varkappa)$:

$$K = \frac{D^2P - DP^2}{1 + DP + D^2P^2 + P^2}. \quad (13)$$

Differentiating equation (13) treating D as a constant gives:

$$\frac{dK}{dP} = \frac{D(D - 2P - 2DP^2 - D^3P^2)}{(1 + DP + D^2P^2 + P^2)^2}. \quad (14)$$

Table 2. Conditions for maximum values of $\varkappa$ for $\psi > 0$

δ_o	ψ	δ	θ	$\varkappa$
75	13.2	61.8	61.8	48.6
70	16.1	53.9	53.9	37.9
65	18.0	47.0	47.0	29.0
60	19.1	40.9	40.9	21.8
55	19.5	35.5	35.5	16.1
50	19.2	30.8	30.8	11.6
45	18.4	26.6	26.6	8.1

For each δ_o, the value of ψ for maximum $\varkappa$ is calculated using equation (17). The value of δ is then calculated as $\delta_o - \psi$; θ is then calculated using equation (6); and $\varkappa$ is calculated as $\theta - \psi$.

Apart from the solution with $D = 0$ ($\delta_o = 0°$), dK/dP will be zero, at a maximum, when:

$$P^2(D^3 + 2D) + 2P - D = 0 \qquad (15)$$

or

$$P = \frac{-1 \pm (D^2 + 1)}{D(D^2 + 2)}. \qquad (16)$$

Positive values of ψ are relevant to the tilting of normal faults during extension. The positive root of equation (16) is thus appropriate:

$$\tan(\psi) = \frac{\tan(\delta_o)}{\tan^2(\delta_o) + 2}. \qquad (17)$$

Values of ψ corresponding to maximum $\varkappa$ for different values of δ_o are listed in Table 2, with corresponding values of δ, θ and $\varkappa$. Maximum $\varkappa$ occurs when $\delta = \theta$ for the values of δ_o listed. It is easy to show that this is true in general, and is so because the condition for maximum $\varkappa$ for normal faults with $\psi > 0°$ corresponds to $\tan(\delta) = \tan(\delta_o)/2$.

As already noted, $\varkappa$ is zero when a normal fault tilts to zero dip. If a normal fault were to tilt through the horizontal direction, reversing its dip polarity, $\varkappa$ would be negative.

The negative root of equation (16) is:

$$\tan(-\psi) = \cot(\delta_o). \qquad (18)$$

This solution is appropriate to any fault that becomes steeper as a result of vertical shear in its surroundings. The extent to which it can be considered applicable to reverse-faulting is briefly discussed later. It is noteworthy that equation (18) is not equivalent to equation (17) with a change of sign. In particular, because equation (18) corresponds to $\psi = \delta_o - 90°$, it gives $\delta = 90°$ regardless of δ_o. Thus this second solution involves $\varkappa$ increasing monotonically as fault dip increases to 90° (Table 3) except for $\delta_o = 0°$ when $\varkappa$ is always 0°.

Vertical shear and rigid-body rotation thus predict fundamentally different relationships between fault and bed tilting. The difference $\varkappa$ can be substantial for normal faults with initial dip $\gtrsim 50°$ (Tables 1 and 2), which should enable these two schemes to be distinguished by field data.

Table 3. Reverse fault and bed tilting assuming distributed vertical simple shear

Fault tilt ($\psi = \delta_o - \delta$)	Bed tilt (θ)	$\varkappa = (\theta - \psi)$
	$\delta_o = 0°$	
0.0	0.0	0.0
−7.5	−7.5	0.0
−15.0	−15.0	0.0
−22.5	−22.5	0.0
−30.0	−30.0	0.0
−37.5	−37.5	0.0
−45.0	−45.0	0.0
−52.5	−52.5	0.0
−60.0	−60.0	0.0
−67.5	−67.5	0.0
−75.0	−75.0	0.0
−82.5	−82.5	0.0
−90.0	−90.0	0.0
	$\delta_o = 15°$	
0.0	0.0	0.0
−7.5	−8.3	−0.8
−15.0	−17.2	−2.2.
−22.5	−26.5	−4.0
−30.0	−36.2	−6.2
−37.5	−46.0	−8.5
−45.0	−55.7	−10.7
−52.5	−65.0	−12.5
−60.0	−73.9	−13.9
−67.5	−82.2	−14.7
−75.0	−90.0	−15.0
<−75.0	impossible	
	$\delta_o = 30°$	
0.0	0.0	0.0
−7.5	−10.8	−3.3
−15.0	−22.9	−7.9
−22.5	−36.0	−13.5
−30.0	−49.1	−19.1
−37.5	−61.4	−23.9
−45.0	−72.4	−27.4
−52.5	−81.9	−29.4
−60.0	−90.0	−30.0
<−60.0	impossible	
	$\delta_o = 45°$	
0.0	0.0	0.0
−7.5	−16.9	−9.4
−15.0	−36.2	−21.2
−22.5	−54.7	−32.2
−30.0	−69.9	−39.9
−37.5	−81.4	−43.9
−45.0	−90.0	−45.0
<−45.0	impossible	
	$\delta_o = 60°$	
0.0	0.0	0.0
−7.5	−34.3	−26.8
−15.0	−63.4	−48.4
−22.5	−80.3	−57.8
−30.0	−90.0	−60.0
<−30.0	impossible	
	$\delta_o = 75°$	
0.0	0.0	0.0
−7.5	−75.5	−68.0
−15.0	−90.0	−75.0
<−15.0	impossible	

See text for discussion.

VERTICAL SHEAR OR BLOCK ROTATION? SOME OBSERVATIONS

We now compare and contrast the angular relationships expected for distributed vertical simple shear and rigid-body rotation for normal faults in western Turkey,

Table 4. Fault and bed dips

Fault	Block	δ	θ	δ_{oS}	δ_{oR}	$\varkappa$	C
Western Turkey							
Denizli	F	45	20	54	65	9	0.32
Büyük Menderes	F	45	26	56	71	15	0.40
Western United States							
Tucki Mountain	H (1a)	30	21	44	51	7	(0.03)
Tucki Mountain	F + H (1b)	18	39	49	57	8	0.14
[Tucki Mountain	F + H (2)	18	50	57	68	11	0.45]
Cricket Mountain	F + H	52	20	59	72	13	0.53
Wasatch	F	45	35	60	80	20	0.58
Virgin Mountains	H	60	19	64	79	15	0.78
[Virgin Mountains	F (1)	60	45	70]			
[Virgin Mountains	F (2)	60	60	74]			
North Sea							
Draugen	F + H	47	13	53	60	7	0.29
Coffee Soil	H	52	16	57	68	11	0.45
Eastern Atlantic Margin							
Outer Isles	H	25	18	38	43	5	(0.25)
West Shetland	F + H	43	22	53	65	12	0.29

F and H denote footwalls and hanging-walls of faults. Angles δ and θ denote present-day dips of faults and adjacent beds; δ_{oS} is the estimate of initial fault dip δ_o assuming vertical shear (equation 6); δ_{oR} is the estimate assuming rigid-body rotation (equation 1); and $\varkappa$ is the difference between δ_{oS} and δ_{oR}. C is the estimate of coefficient of friction using equation (19). Values in parentheses are for faults with $\delta_{oS} < 45°$, calculated assuming they are reactivated reverse faults. Alternative solutions, which we do not prefer, are in brackets. For the Virgin Mountains fault, these are from Wernicke & Axen's (1988) cross-section: (1) derives θ assuming their value of δ_{oS}; and (2) derives δ_{oS} assuming their value of θ. In both cases, no solution is possible for rigid-body rotation. Solution (1) for Tucki Mountain assumes the first generation of fault took up extension until its dip reduced to 30° (a), after which the second generation took over (b). Solution (2) assumes all tilting has accompanied the second generation of faulting.

in the Basin and Range province of the western United States, and in the North Sea. Our strategy has been to select faults whose surroundings tilt at angles that correspond to substantial $\varkappa$, bearing in mind Table 2. Many other normal faults exist where $\varkappa$ is small, but these are less useful for distinguishing rigid-body rotation from vertical shear.

Some of these case studies show uniform tilting between the fault being considered and other faults up to ~10 km away, revealing blocks that could be described either as rigid 'dominoes' or as undergoing uniform vertical shear. Others comprise isolated normal fault zones in whose surroundings tilt decreases gradually to zero. In the cross-sections that are based on fieldwork (the examples from Turkey, and the Virgin Mountains, Wasatch and Tucki Mountain faults in the western United States), the major faults show en échelon branches ~1–2 km apart, which bound blocks that could be described either as rigid 'dominoes' or as undergoing uniform vertical shear (Fig. 3). Such features have not been reported in some of the examples studied by seismic reflection. However, it is difficult to image steep features such as a normal faults using normal-incidence seismic profiling at all (e.g. Yielding *et al.* 1991), let alone with the detail necessary to reveal such close en échelon fault branches. Whether or not such close branches are present in these cases, their overall form can also potentially be described as the result of either rigid-body rotation or vertical shear.

Anderson's (1951) theory of faulting holds that dip-slip faults initiate with the dip δ_o that minimizes horizontal deviatoric stress. For faults that cut the brittle layer, this satisfies:

$$\cot(2\delta_o) = nC, \tag{19}$$

where C is the coefficient of friction on the fault and n is +1 for reverse faults and −1 for normal faults (see e.g., Turcotte & Schubert 1982, pp. 354–355). For normal faults, Jackson's (1987) suggestion that δ_o is typically 60° implies $C = 0.58$. Turcotte & Schubert (1982, p. 353) suggested that C is typically ~0.85 in laboratory rock-mechanics studies (see also Byerlee 1978), which would predict $\delta_o = 65°$. A frictionless fault with $C = 0$ would have $\delta_o = 45°$; a normal fault with $C = 1$ would have δ_o, $= 67.5°$. This theory thus predicts a limited range of initial dips for major normal faults, from $\gtrsim 45°$ to $\gtrsim 65°$. We use it to establish likely bounds for initial dip of normal faults for comparison with observations (Table 4).

Western Turkey 1: *Denizli basin*

The Denizli Neogene extensional sedimentary basin in western Turkey is described by Westaway (1993). It is situated between the eastern end of the Büyük Menderes fault zone that has taken up much of the Neogene and Quaternary extension of westernmost Turkey (Westaway 1990a) and the eastern edge of the extensional province (Fig. 5a). Parts of its interior are an active depocentre, as a result of hanging-wall subsidence;

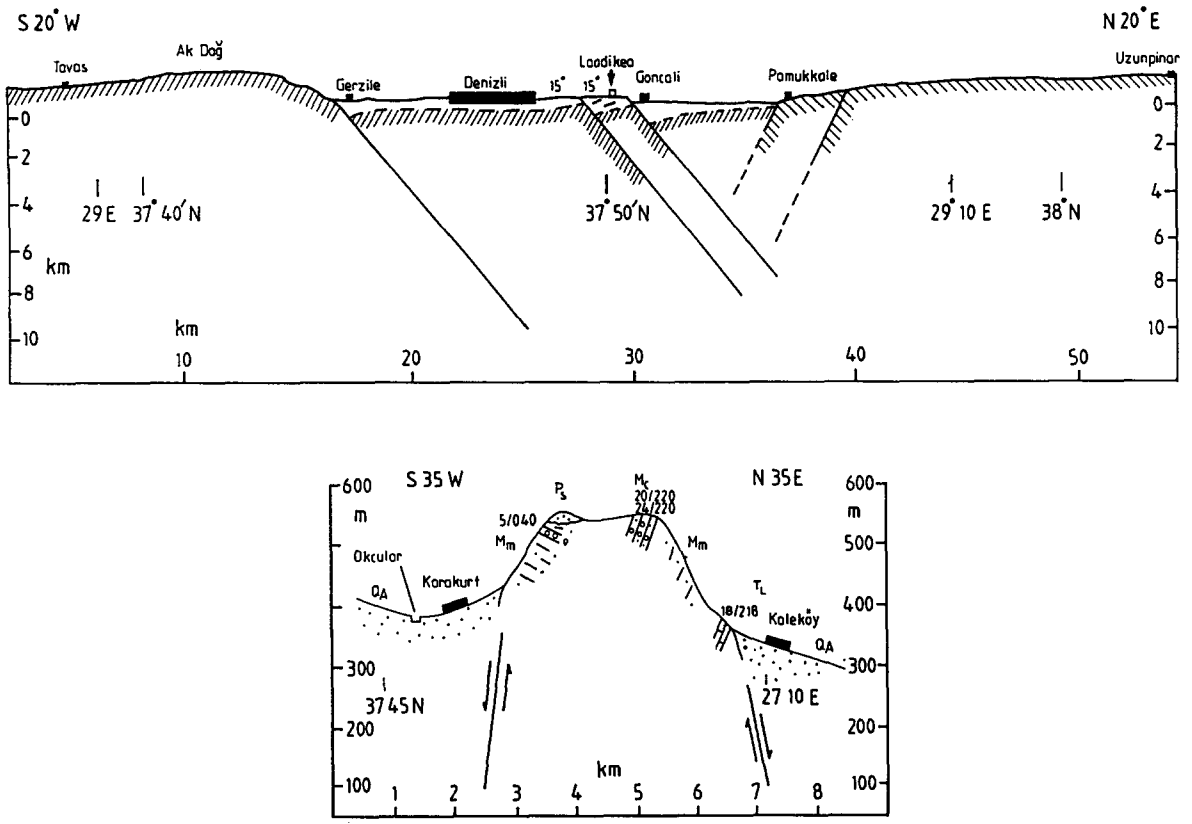

Fig. 5. Cross-sections across the Denizli basin in western Turkey. (a) Cross-section across the central part of this basin; fig. 7(c) of Westaway (1993). Diagonal shading indicates pre-extensional basement. (b) Cross-section across the eastern part of this basin, adapted from fig. 4 of Westaway (1993) to show the preferred interpretation of local structure. Upper Miocene rocks are interpreted as: T_L, Tortonian limestone; M_m, Messinian marl; and M_c, Messinian conglomerate. P_s and Q_A are Pliocene sand and Quaternary alluvium.

other parts have uplifted in the footwalls of normal faults within the basin (Westaway 1993).

The maximum dip of exposed sediment in the uplifted footwalls of normal faults within the basin is ~20° (Fig. 5). Taking 45° as a lower limit for the present-day dip of these normal faults (see Westaway 1993), rigid-body rotation predicts initial dip of 65°, and vertical shear predicts 54°. This estimate for rigid-body rotation is rather high, but cannot be excluded. As is discussed by Westaway (1993), other aspects of the form of this basin support vertical shear. In particular, the thinness of the sedimentary sequence in relation to the substantial tilting, and the observed reversal in polarity of tilting over a few kilometres distance (Fig. 5b) preclude rigid-body rotation.

Western Turkey 2: Büyük Menderes fault zone

Given that the Neogene extension increases westward across western Turkey, greater amounts of bed tilting are expected beside faults farther west. Jones & Westaway (1991) have studied part of the Büyük Menderes normal fault zone near Germencik, ≥100 km west of Denizli. This fault zone locally has two principal en échelon branches ~4 km apart (Fig. 6). The seismically-active southern branch, in whose footwall basement is exposed, has 45° dip at the Earth's surface. An active depocentre exists in its hanging-wall, and Neogene sediments of the Arzular basin above exposed basement in its uplifted footwall locally dip north at up to 26°. The northern branch, which may no longer be active, has basement in its uplifted and eroded footwall, with the Arzular basin in its hanging-wall. Assuming that the 4-km-wide block containing the Arzular basin has rotated as a rigid body, an initial normal fault dip of 71° is required. Assuming vertical shear instead, the initial normal fault dip would be 56°.

Western United States 1: Virgin Mountains fault, northwestern Arizona

The WNW-dipping Virgin Mountains fault passes near the triple junction of Utah, Arizona, and Nevada, in the western United States. Its northern part that is discussed here, in northwestern Arizona, has been the subject of lively debate (Wernicke & Axen 1988, Axen & Wernicke 1989, Carpenter *et al.* 1989) (Fig. 7). According to Axen & Wernicke (1989) this fault has taken up southwestward extension. If so, its extension is strongly oblique, with predominant left-lateral slip. Many differences between published interpretations of this fault zone concern fine details of stratigraphy and local structure, about which we hold no views. We address here instead the first-order features: its present-day dip, and the dip of top basement and major inter-

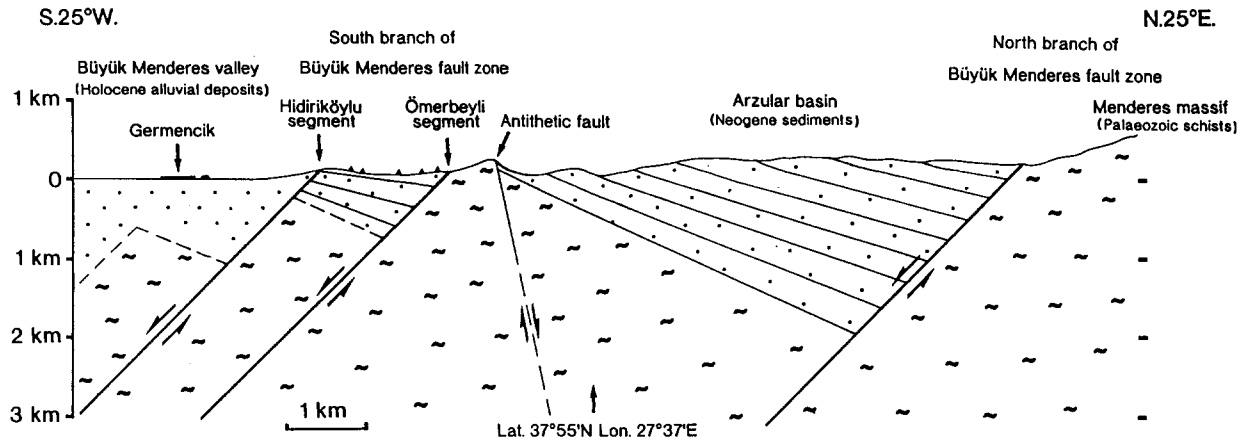

Fig. 6. Cross-section across the Büyük Menderes fault zone at Germencik in western Turkey. Adapted from fig. 3 of Jones & Westaway (1991).

faces within basement, which were presumably subhorizontal when extension began.

Given their scheme for footwall vertical shear, Wernicke & Axen (1988) drew a cross-section mainly within the Virgin Mountains fault footwall (Fig. 7a). This showed the fault dipping at ~60° at the Earth's surface, with bed tilt varying smoothly within its footwall with a maximum (~4 km from the fault) ~60°. It would be consistent with vertical shear with an initial fault dip of ~74°. Their restoration (Fig. 7b) shows an initial fault dip of 70°, which would be consistent with vertical shear with ~45° of tilting beside the fault. As already noted, it is fundamental to the assumption of vertical shear that initially steep features such as faults, and initially flat surfaces in general, tilt by different angles. Careful inspection of Wernicke & Axen's (1988) figures indicates that they have restored cross-sections assuming instead that angular relationship are preserved. In terms of our notation, they have mistakenly assumed that $\varkappa$ is always zero for distributed vertical simple shear. Their method for restoring cross-sections is thus inconsistent with their general scheme that assumes vertical shear.

The cross-section by Carpenter *et al.* (1989) (Fig. 7c) has roughly the same position and orientation as Fig 7(a). The footwall in Fig 7(c) is constrained by mapping; the hanging-wall is a seismic reflection time section. Both parts are also constrained by gravity, the Bouguer anomaly in the hanging-wall basin being −52 mgal. This is consistent with ~5 km typical sediment thickness with density contrast $-300\ \mathrm{kg\ m^{-3}}$. Over 5 km, the horizontal distance two-way time for the reflection from top basement increases from 2.7 to 3.8 s. Assuming uniform seismic velocity of $3\ \mathrm{km\ s^{-1}}$ in the sediment, the depth of this reflector increases from ~4 to ~5.7 km, the latter depth being at a point within ~2 km of the cutoff of top basement at the Virgin Mountains fault. This ~1.7 km of tilting over 5 km distance gives a local average dip of top basement of ~19°. Carpenter *et al.* (1989) agree with Wernicke & Axen (1988) that the Virgin Mountains fault now dips at ~60°. Assuming vertical shear, these hanging-wall observations give its initial dip of 64°, whereas assuming rigid-body rotation gives 79° instead.

The dramatically different amounts of tilt on opposite sides of the Virgin Mountains fault are thus consistent with similar initial fault dips. However, the cross-section by Carpenter *et al.* (1989) does not show smooth variations in footwall tilting. Instead, it shows markers broken by numerous minor faults into short segments with very different dips. Wernicke & Axen (1988) appear to have interpolated these segments to obtain their smoother profile. Because of this potential problem, our preference is for the parameters derived from analysis of Carpenter *et al.*'s (1989) profile of the hanging-wall (Table 4).

Western United States 2: *Cricket Mountain fault, western Utah*

The Cricket mountain fault in western Utah has been studied by Stein *et al.* (1988) because it shows very clear footwall and hanging-wall tilting. This is because it is situated in an internally draining basin where rapid sedimentation has buried the hanging-wall and much of the footwall (Fig. 8). A basalt flow in the footwall causes a distinctive seismic reflector, and a similar reflector in the hanging-wall is interpreted as a continuation of the same unit. This flow, which was presumably subhorizontal when it formed at 4.2 Ma, now tilts at 20° in both the footwall and hanging-wall; the fault now dips at 52°. The fault dip when the flow formed was thus 59° assuming vertical shear, or 72° assuming rigid-body rotation. Stein *et al.* (1988) suggested that the beds beneath this reflector pre-date the faulting. These values are thus estimates of the initial dip of the fault. If this suggestion is wrong, then the fault presumably became active some time before 4.2 Ma, and these estimates are thus lower bounds for its initial dip.

Western United States 3: *Wasatch fault, central Utah*

The Wasatch fault is probably the best-known active normal fault in the western U.S.A., and is also one of the most important, with a heave of more than 10 km (e.g. Wernicke & Axen 1988). Much of the footwall uplift

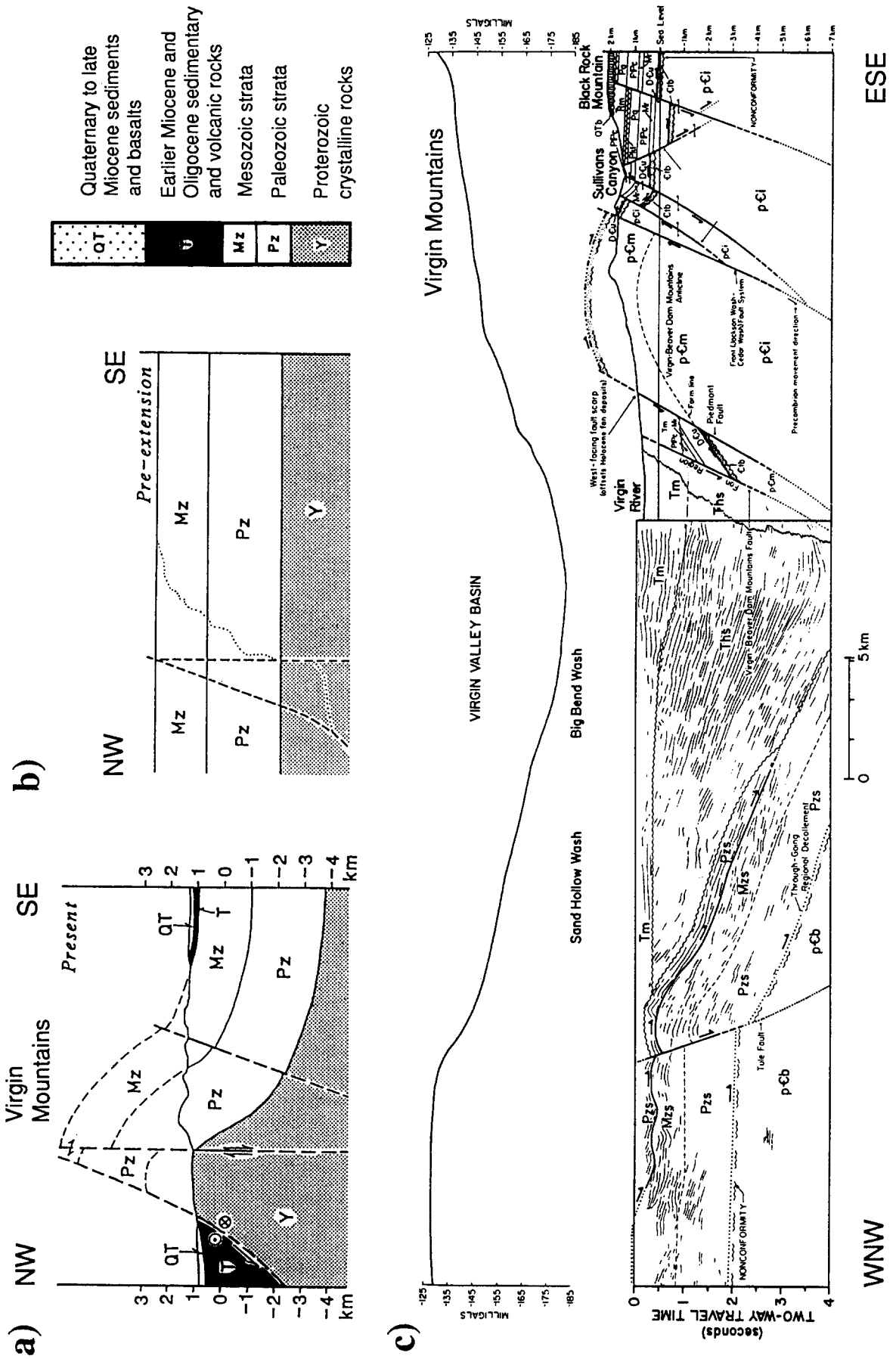

Fig. 7. Cross-sections across the Virgin Mountains fault in northwestern Arizona. (a) Present-day form as suggested by Wernicke & Axen (1988), adapted from their fig. 2(c), with no vertical exaggeration. (b) Restoration of dip-slip as suggested by Wernicke & Axen (1988), adapted from their fig. 2d, also with no vertical exaggeration. Dotted line denotes the restored position of the present-day Earth's surface. For other symbols see legend to (a). Note that this restoration preserves angles. (c) Present-day form as suggested by Carpenter *et al.* (1989), adapted from their fig. 1. Axen & Wernicke (1989) suggested that this cross-section is 'rather similar' to (a), although inspection reveals substantial differences.

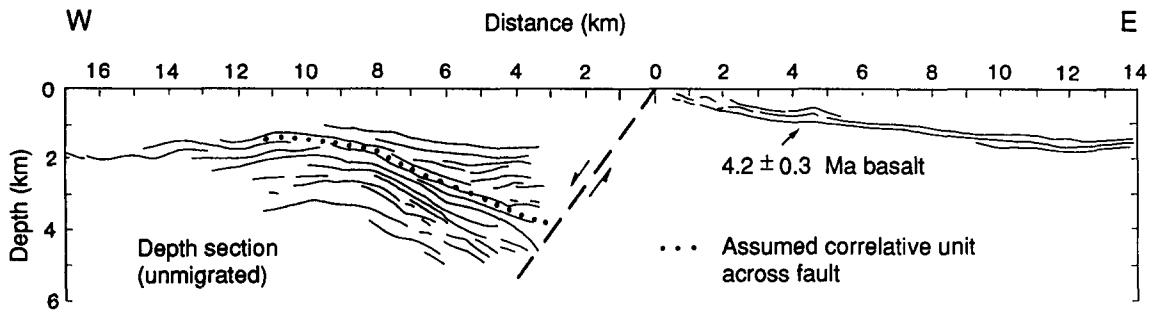

Fig. 8. Cross-section across the Cricket Mountain fault in western Utah. Adapted from fig. 8(b) of Stein *et al.* (1988).

that has accompanied extension across it has been lost by erosion, but is revealed by both analysis of fluid inclusions (e.g. Parry & Bruhn 1987), and structural studies (Fig. 9). The cross-section in Fig. 9 shows a present-day fault dip of 45°, with footwall basement dipping at up to 35°. Assuming vertical shear, the initial dip of the Wasatch fault was 60°. Assuming rigid-body rotation, its initial dip was 80°. More detailed studies by Bruhn *et al.* (1987) reveal exposures of the Wasatch fault at nearby localities with dip more typically ~35°, rather than 45°, as in Fig. 9. If considered more typical, this lower present-day dip requires an initial dip of 54° for vertical shear, or 70° for rigid-body rotation.

Western United States 4: *Tucki Mountain fault, California*

The Tucki Mountain fault zone in eastern California shows dramatic tilting associated with extreme E–W extension since Oligocene time (Fig. 10). It is an example of a metamorphic core complex, and has been studied by Hamilton (1987) and others. It comprises a low-angle convex-upward 'detachment' whose eastern part dips east at ~13°, which separates underlying Precambrian metamorphic rock from unmetamorphosed Palaeozoic rock in the overlying 'upper plate'. Beds in this upper plate dip east at about 50°, and are cut by closely-spaced normal faults that dip west at about 18°. The detachment is believed to be a normal fault that has tilted through the horizontal direction in the east, such

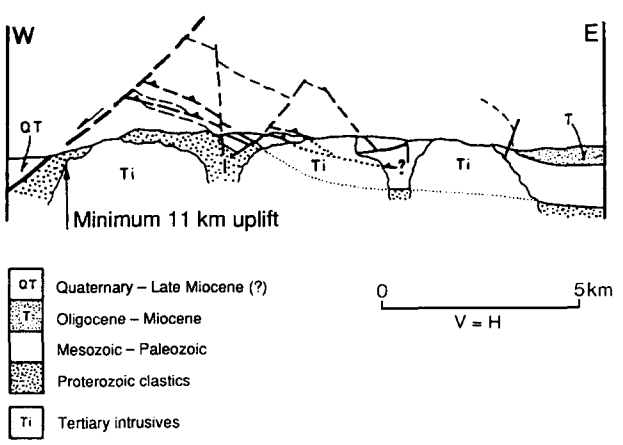

Fig. 9. Cross-section across the Wasatch fault in the Cottonwood Canyon area of central Utah. Adapted from fig. 3(a) of Wernicke & Axen (1988).

that its dip polarity has reversed. Hamilton (1987) suggested that the detachment was the first generation of normal fault to be active, and the normal faults that cut the upper plate and sole into it are a younger, second generation of faulting.

Accepting this view, one may restore the tilt of the detachment, the later normal faults and the beds. If *all* tilt of the observed beds is assumed to relate to displacement on the late normal faults, then for vertical shear these faults had an initial dip of 57°. Following this assumption, the vertical shear strain accompanying extension is 1.19 (tan 50°). The detachment would have thus initially dipped west at 44° (solution 2 in Table 4), such that its orientation has changed during extension by 57° (44° minus −13°). Note that this solution makes $\varkappa = -7°$ for the detachment. Such a negative value is expected after a reversal of dip polarity, in accordance with equation (12) for $\psi > \delta_0$. For rigid-body rotation, the later normal faults initiated with dip 68°, when the detachment dipped west at 37°.

These dip values for the second generation of faults are upper limits, because some of the bed tilting may have occurred during the first generation of faulting. If the 30° dip limit suggested by Jackson & McKenzie (1983) applied to the first generation of normal faults at Tucki Mountain, then assuming vertical shear this fault zone evolved as follows. The detachment initiated with a westward dip of 44° and took up extension until this dip reduced to 30° (solution 1a in Table 4). At this time the beds now exposed in its hanging-wall, the present-day upper plate, would have dipped east at 21°, corresponding to vertical shear strain 0.38. The later normal faults formed with dip 49° (solution 1b in Table 4), and subsequent extension within the upper plate has tilted them, the surrounding beds, and the detachment, to their present orientations. The vertical shear strain during this second phase of faulting is estimated as 0.81, [tan(30°) − tan(−13°)]. A bed deposited at the start of this phase would thus now dip at 39°; hence $\theta = 39°$ in Table 4. The observed beds, which at the start of this phase are estimated to have tilted at 21°, thus increased their tilt by 29°. Table 4 summarizes this alternative solution (1), which predicts that *most* of the vertical shear strain developed during the second generation of faulting, and its equivalent for rigid-body rotation. Note that the total vertical shear strain is the same under both interpretations. The predicted initial dip of the detach-

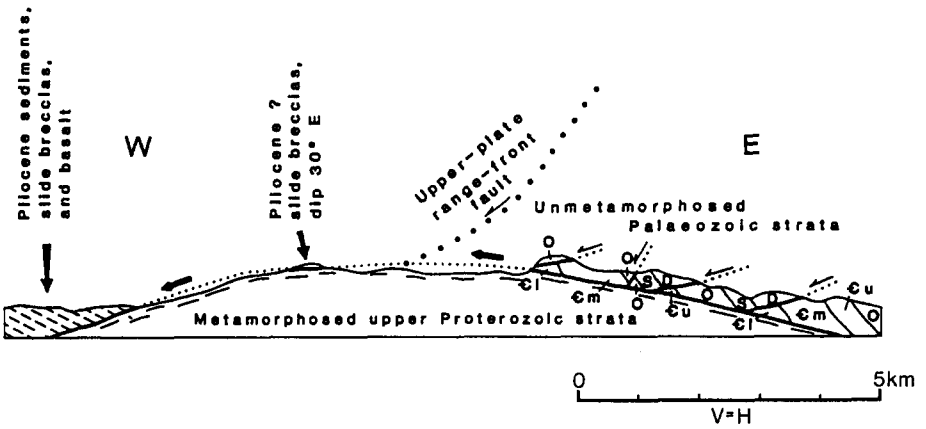

Fig. 10. Cross-section across the Tucki Mountain fault zone in eastern California, adapted from fig. 20 of Hamilton (1987). Slip sense on the subhorizontal 'detachment' was top-to-the-west. Cl, Cm and Cu are Lower, Middle and Upper Cambrian rocks; O, S and D are Ordovician, Silurian and Devonian.

ment is thus also the same, regardless of how much tilting was associated with extension on it. However, the predicted initial dip of the second set of faults varies between interpretations. The predicted 44° initial dip of the detachment is too small to satisfy equation (19) as a normal fault. It supports this feature having formed as a reverse fault instead, and having been later reactivated as a normal fault. Many people (e.g. Coney & Harms 1984) have indeed suggested that metamorphic core complexes in the western United States formed in the footwalls of normal faults that are reactivated older reverse faults.

North Sea 1: *Coffee Soil fault, Danish sector of southern North Sea*

The Coffee Soil fault is one of the most significant normal faults in the southern North Sea, with ~7 km of observable throw, plus more that may have been lost by erosion of its uplifted footwall. It has been studied by Roberts & Yielding (1991) (Fig. 11), and the dip of its fault plane is well-constrained at 52° by seismic reflection. The top Rotliegend (i.e. uppermost Lower Permian) reflector, which pre-dates the local Triassic and Jurassic extension, dips at 16° in the hanging-wall (Fig. 11). Vertical shear predicts initial fault dip 57°; rigid-body rotation predicts 68° instead. The Coffee Soil fault offsets Paleozoic basement, which is unlikely to have compacted following burial after extension ceased. Estimates of fault dip are thus unlikely to be affected by such compaction, unlike many other normal faults in the North Sea (e.g. Yielding *et al.* 1991).

North Sea 2: *Draugen fault, Norwegian sector of northern North Sea*

The Draugen fault in the northern North Sea was also studied by Roberts & Yielding (1991) (Fig. 12). Its dip is now 47°. The top Lower Triassic reflector, which pre-dates the Upper Triassic and Jurassic extension, dips towards the fault at 13° in the hanging-wall and away from it at a similar angle in the smoothed profile through the footwall (Fig. 12). The vertical shear model predicts an initial fault dip of 53°, whereas rigid-body rotation predicts 60°. At least part of the displacement on the Draugen fault offsets Lower Triassic sediment that was probably unconsolidated when the fault was active. Any subsequent compaction of this sediment will have reduced the fault dip (e.g. Yielding *et al.* 1991). The result that the Draugen fault has smaller estimated

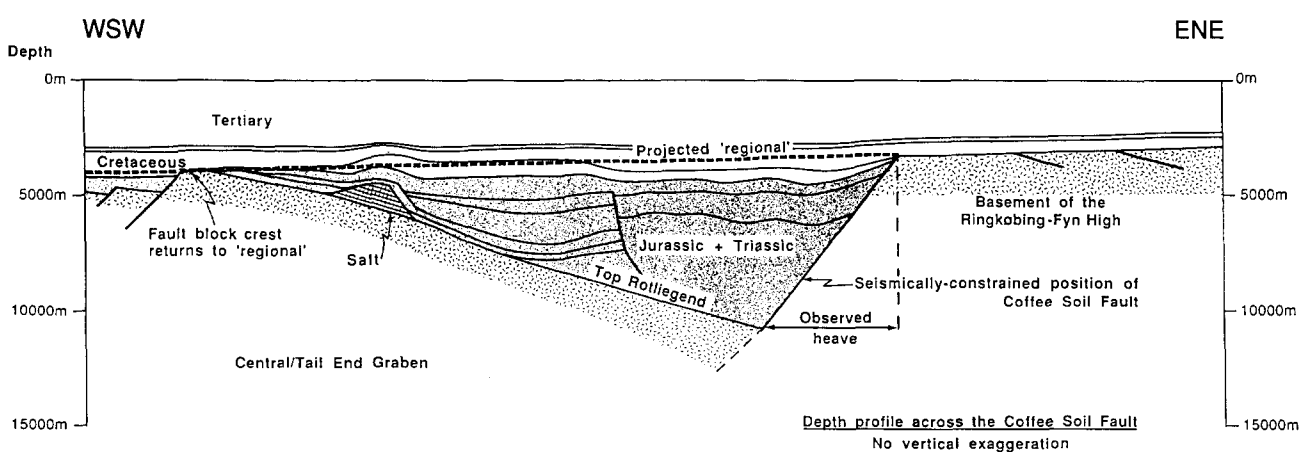

Fig. 11. Cross-section across the Coffee Soil fault in the Danish sector of the southern North Sea, adapted from fig. 4 of Roberts & Yielding (1991).

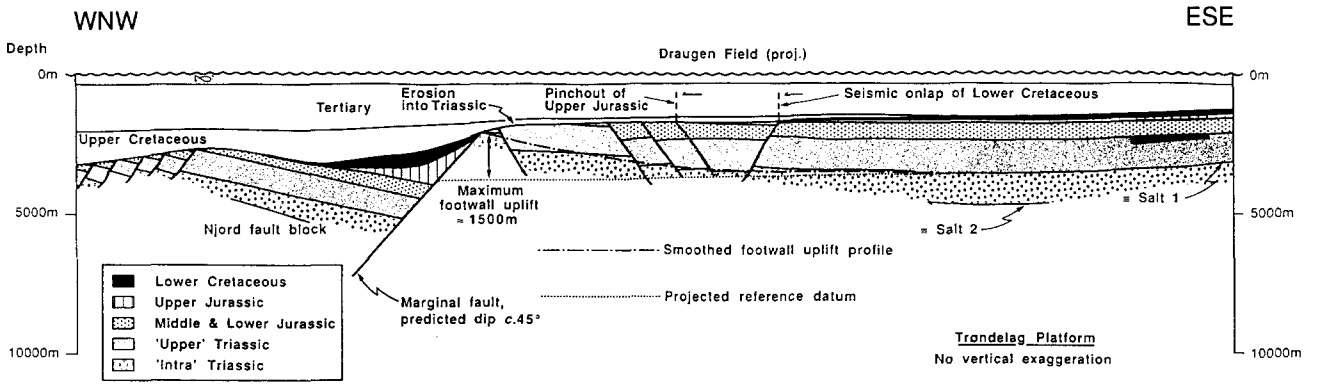

Fig. 12. Cross-section across the Draugen fault (also known as the Halten Terrace basin marginal fault) in the Norwegian sector of the northern North Sea, adapted from fig. 6 of Roberts & Yielding (1991).

initial dip than most other normal faults considered (Table 2) may to some extent reflect this process.

Summary of results

The assumption of distributed vertical simple shear predicts initial dips of normal faults that resemble the ~60° typical value for normal faults elsewhere (Jackson 1987). In contrast, the assumption of rigid-body rotation predicts very large initial dips for some faults, with no solution possible in some cases (see, e.g., Westaway *et al.* 1989, or Table 4). On the basis of consistency of initial dips the assumption of vertical shear is preferable.

DISCUSSION

Initial dips of normal faults

The normal faults examined above favour distributed vertical simple shear rather than rigid-body rotation as the cause of the observed tilting. Following this assumption, initial dips of normal faults straddle 60°. For the Denizli example, our preference for vertical shear is mainly to explain the substantial tilting of beds in a thin extensional basin, and the reversals of fault and tilt polarity within the basin (Fig. 5b). In most other cases it is because the alternative assumption of rigid-body rotation predicts initial fault dips that are unrealistically large. In some localities, the typical initial fault dip assuming vertical shear is smaller than 60°, nearer 55° instead, particularly in the North Sea and western Turkey (Table 4). Although small, the difference between 55° and 60° may be important to people who model extension elsewhere, and who work without independent evidence of initial fault dip. If the true deformation style in the surroundings of any normal fault is vertical shear, then restoring fault tilting assuming it equals bed tilting will overestimate initial fault dip.

In the North Sea, where not much extension has occurred and the observed tilting of beds is gentle, estimates of initial fault dip assuming rigid-body rotation are not unreasonable. However, the larger tilts of beds in western Turkey and the western United States are much more difficult to reconcile with rigid-body rotation. Most estimates of initial fault dip are slightly higher for the western United States than for the North Sea and western Turkey. This contrasts with the popular view that the Basin and Range province contains 'low-angle' normal faults. Although some normal faults in the western United States now have very low-angle dips (e.g. Fig. 10), these appear to have developed from much steeper intital dips following substantial extension. Some small normal faults initiate with much steeper dip of ~80°, instead, whereas others initiate no steeper than ~40°. Table 1 of Westaway (1993) lists examples from western Turkey. Evidently there is no unique dip for normal faults of all sizes, even in this restricted region. However, excluding the Tucki Mountain case study, where an initial fault dip cannot be uniquely resolved because of the two generations of faulting, the range of initial dip values of normal faults for vertical shear is only 11° (Table 4), from 53° to 64°, with average 57° for the seven faults considered. Using equation (19) this corresponds to a coefficient of friction of 0.29–0.78, with an average of 0.48 ± 0.16.

Estimates of extension for vertical shear and rigid-body rotation

It is interesting to compare estimates of extension assuming rigid-body rotation and vertical shear. 'Rigid-domino' extension leads to simple relationships between extensional strain ε (where $\varepsilon = \beta - 1$, β being the extension factor), heave H, throw T, and dip δ, for faults with a given initial dip δ_o, initial spacing W_o, and present-day spacing W:

$$\varepsilon = \sin(\delta_o)/\sin(\delta) - 1 \quad (20)$$

$$W = W_o \sin(\delta_o)/\sin(\delta) \quad (21)$$

$$H = [W\cos(\delta) - W_o \cos(\delta_o)]\cos(\delta) \quad (22)$$

(see, e.g., Westaway *et al.* 1989).

Suppose a region contains many normal faults with initial separation W_o = 10 km, which now form an indefinite profile with sawtooth topography, with fault

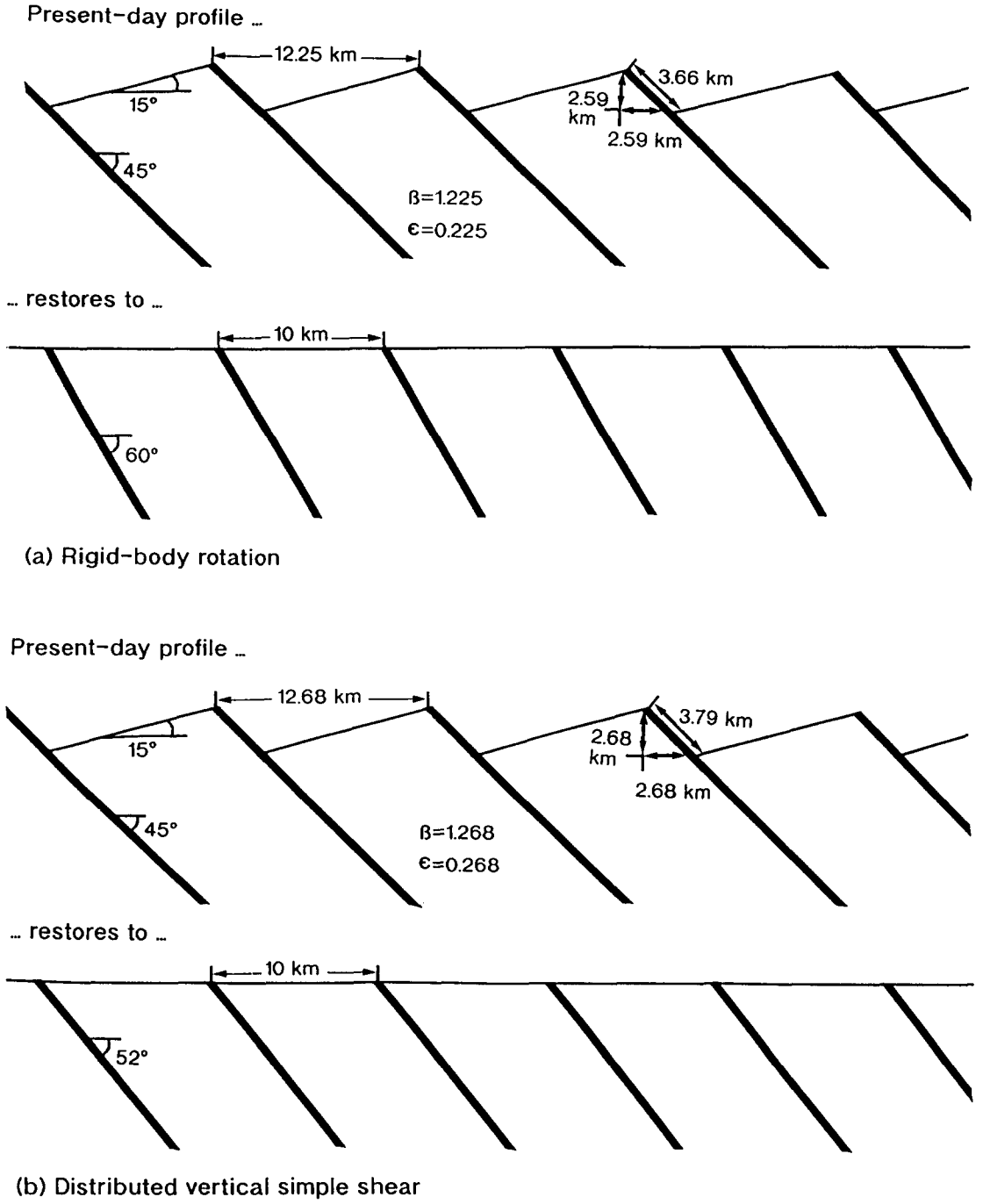

Fig. 13. Comparison of the consequences of rigid-body rotation (a) and vertical shear (b) for close, equispaced, normal faults. All cross-sections are drawn true to scale, with no vertical exaggeration.

dip $\delta = 45°$ and dip of intervening beds (θ) uniformly 15°. Heave and throw are the same for, and topography is identical across, every fault in each of the profiles (Fig. 13).

For vertical shear, the heave on each fault equals the extension across it. Initial fault dip is 52° (equation 6), and the difference in elevation of the two ends of a bed, from the hanging-wall cutoff at one fault to the footwall cutoff at the next, is $W_0 \tan(\theta)$ or 2.68 km. The throw on each fault is thus 2.68 km, and, given the 45° dip, so is the heave: fault displacement is 3.79 km, $\varepsilon = 0.268$ and $\beta = 1.268$.

Extension for rigid-body rotation can be estimated from ε, which depends only on fault dips. Thus, δ_0 is $\delta + \theta$ or 60°, making $\varepsilon = 0.225$ and $\beta = 1.225$. The separation of equivalent points (say, footwall cutoffs of top basement) for adjacent faults is thus now 12.25 km, indicating 2.25 km of extension per fault. Equation (22) predicts instead 2.59 km of heave and throw per fault for rigid-body rotation, making fault displacement 3.66 km. Although this fault displacement differs minimally from the value for vertical shear, the extension for vertical shear substantially exceeds the value for rigid-body rotation. These structures generated by rigid-body rotation and vertical shear thus have identical fault and bed dips and only tiny differences in heave and throw.

However, assuming vertical shear predicts substantially (~20%) more extension than assuming rigid-body rotation.

Rotation of normal faults through the vertical direction

Jackson *et al.* (1982) have discussed possible explanations for observations of minor reverse faults near major normal faults in extensional regions such as Greece. They suggest that these faults formed as steep normal faults, then rotated through the vertical during extension on the nearby major normal faults, and now look like reverse faults instead. However, if tilting in the surroundings to any normal faults is by vertical shear, no marker in these surroundings can pass through the vertical, and this mechanism is no longer a possible explanation for these features. Minor reverse faults are shown in Fig. 7(c) near the Virgin Mountains normal fault. Reverse-faulting aftershocks have been noted near other major normal faults that slip in large normal-faulting earthquakes (e.g. Westaway & Jackson 1987), and require minor active reverse faults. It may thus not be unreasonable to expect minor reverse faults in the surroundings of other major normal faults also, although these do not imply regional shortening. Vertical shear can of course readily tilt normal faults through the *horizontal* direction, as in Fig. 10.

Implications for studies of the surroundings of normal faults

Our analysis has implicitly regarded the brittle upper crust in the surroundings of each normal faults as a continuum at the scale of our cross-sections. In reality, strain in these surroundings is likely to become localized on small-scale structures when examined on a fine enough scale, which may thus provide a field test for vertical shear. Ramsay (1967, pp. 83–91) discussed angular relationships associated with distributed simple shear, and suggested forms of small-scale structures that may accommodate it.

Field tests for vertical shear have examined the highly deformed surroundings to normal faults that have taken up very large amounts of extension, with footwalls that have uplifted from mid-crustal depths. For example, Bartley *et al.* (1990) studied the footwall of one example in eastern California. They concluded that the observed deformation favours flexure, not vertical shear, as its cause. However, Axen & Wernicke (1991) have reinterpreted their results, arguing that a subvertical mylonitic fabric in this uplifted footwall favours vertical shear instead. Where extension is moderate and curvature in the surroundings of a normal fault is gentle, flexure and vertical shear can be expected to be more difficult to distinguish in the field. Flexure requires horizontal contraction, and thus bed-length contraction, near the Earth's surface in the footwall, and horizontal dilation in the hanging-wall. Ideal vertical shear instead preserves length in the horizontal direction, but requires dilation parallel to the Earth's surface of every part of any profile that is tilted, and will thus cause bed-length dilation in both footwall and hanging-wall. The main difference is thus that in the footwall, flexure predicts bed-length contraction but ideal vertical shear predicts bed-length dilation. However, we are not aware of any convincing published field test for vertical shear using this criterion. As already noted, where curvature of the surroundings to a normal fault is gentle, with radius of curvature large compared with the horizontal extent of tilting, the deflection predicted by flexural schemes is predominantly vertical. It thus approximates ideal vertical shear, predicting similar angular relationships between fault and bed tilting, which as we have shown differ from the predictions for rigid-body rotation.

Tilting by vertical shear will not affect the orientation of any feature that is initially vertical, such as a dyke. If tilted bedding cut by a subvertical dyke is observed in the surroundings of a normal fault, one thus cannot validly infer that the dyke is younger than the displacement on the normal fault that caused the tilting. This geometrical property of vertical shear thus has important implications for investigations of the relative timing of normal faulting and magmatism in extensional provinces. It may also enable an unequivocal field test for vertical shear.

Relationships between normal faults and reverse faults

Normal and reverse faults in basement presumably form with dips that are controlled by equivalent rheological criteria, such as those embodied in equation (19). For plausible coefficients of friction C, initial dips ~25–45° for reverse faults and ~45–65° for normal faults are predicted. The subhorizontal reverse faults commonly observed to deform unconsolidated sediments in environments such as accretionary prisms are thus presumably governed by different physics. As an example of a reverse fault in basement, Turcotte & Schubert (1982, pp. 355–356) discussed the Wind River fault in the western United States that has a dip of 35°, from which they estimated $C = 0.36$. However, tilting in basement in its uplifted hanging-wall is up to ~10°. Assuming this tilting was by vertical shear, the initial dip of the fault was ~28°, making $C = 0.67$.

Except for the Tucki Mountain detachment, all normal faults considered so far appear to have formed as normal faults, with initial dip >45°, rather than being reactivated reverse faults. The Outer Isles fault, an east-dipping fault west of northern Scotland on the eastern margin of the north Atlantic, is a good example of reactivation, having formed in Palaeozoic time as a reverse fault before being reactivated in Mesozoic time as a normal fault (see, e.g., fig. 1 of Kusznir *et al.* 1991). Seismic sections reveal its dip as 25°, with 18° dip of top basement beneath its hanging-wall extensional basin. Vertical shear gives a fault dip at the start of extension of 38°; rigid-body rotation gives 43°. Assuming this fault formed as a reverse fault that satisfied equation (19), a 38° dip would correspond to $C = 0.25$. As some increase in its dip may have accompanied the shortening phase, this is an upper bound for the initial dip, and thus a lower

Table 5. Comparison of normal and reverse faults

	Max. $\lvert\varkappa\rvert$	$\lvert\psi\rvert$ for max. $\lvert\varkappa\rvert$	$\lvert\varkappa\rvert$ for $\lvert\psi\rvert = 5°$	$\lvert\varkappa\rvert$ for $\lvert\psi\rvert = 10°$	$\lvert\varkappa\rvert$ for $\lvert\psi\rvert = 20°$
		$C = 0.00$			
Normal fault, $\delta_0 = 45°$	8.1	18.4°	4.1°	6.7°	8.1°
Reverse fault, $\delta_0 = 45°$	45.0°	45.0°	6.9°	13.2°	28.9°
		$C = 0.18$			
Normal fault, $\delta_0 = 50°$	11.6°	19.2°	5.9°	9.4°	11.6°
Reverse fault, $\delta_0 = 40°$	40.0°	50.0°	4.1°	9.4°	21.8°
		$C = 0.36$			
Normal fault, $\delta_0 = 55°$	16.1°	19.5°	8.3°	13.2°	16.1°
Reverse fault, $\delta_0 = 35°$	35.0°	55.0°	2.9°	6.7°	16.1°
		$C = 0.58$			
Normal fault, $\delta_0 = 60°$	21.8°	19.1°	11.9°	18.4°	21.8°
Reverse fault, $\delta_0 = 30°$	30.0°	60.0°	2.0°	4.7°	11.6°
		$C = 0.84$			
Normal fault, $\delta_0 = 65°$	29.0°	18.0°	17.4°	25.6°	28.9°
Reverse fault, $\delta_0 = 25°$	25.0°	65.0°	1.3°	3.2°	8.1°

bound for C. The nearby W-dipping normal faults that took up Mesozoic extension across the West Shetland basin (Fig. 3c) had steeper initial dips: 53° for vertical shear ($C = 0.29$) and 65° for rigid-body rotation. They presumably formed in Mesozoic time as normal faults, as they have the opposite dip polarity to the major Palaeozoic reverse faults in the region. For the small sample considered, roughly the same range of C is thus estimated for both normal and reverse faults (Table 4).

Basement blocks bounded by reverse faults that have taken up small amounts of shortening can resemble rotated dominoes. The set of young, not-very-active reverse faults in Armenia, which were studied by Westaway (1990b), provides a good example. However, many studies of reverse faults in basement that have taken up substantial shortening establish that substantial deformation occurs in their surroundings. The reason why the existence of this deformation has long been recognized for reverse faults, but has been overlooked in many studies of normal faults, may relate to the dramatically different maximum values of $\lvert\varkappa\rvert$ for normal and reverse faults (Tables 1 and 3).

To investigate this possibility, Table 5 compares values of $\lvert\varkappa\rvert$ for different initial dips of normal and reverse faults that form with the same coefficients of friction, given Anderson's (1951) theory. For $C < 0.73$, the maximum $\lvert\varkappa\rvert$ for a normal-fault ($\delta_0 < 63°$) will exceed the maximum $\lvert\varkappa\rvert$ for a reverse-fault ($\delta_0 > 27°$). Most faults considered satisfy this condition for initial dip (Table 4). However, for very small amounts of tilting, $\lvert\varkappa\rvert$ is typically greater for normal faults than for reverse faults. For example, for $\lvert\psi\rvert = 5°$, unless $C < 0.10$, $\lvert\varkappa\rvert$ of normal faults ($\delta_0 < 48°$) will exceed $\lvert\varkappa\rvert$ for reverse faults ($\delta_0 > 42°$). All faults considered satisfy this condition for initial dip. In the early stages, deformation of zones where shortening is taken up on planar reverse faults may thus better approximate rigid-body rotation than where extension is taken up on planar normal faults. However, after substantial shortening or extension has developed, the zone of shortening may approximate rigid-body rotation very badly, but the corresponding zone of extension may still make a reasonable approximation to rigid-body rotation.

This geometrical property of vertical shear makes the investigation of whether it occurs in basement in the surroundings of reverse faults more difficult than in the surroundings of normal faults. For small amounts of shortening $\lvert\varkappa\rvert$ may be minimal and not distinguishable from zero; for large amounts $\lvert\varkappa\rvert$ may be large, but the resulting structures may be so complex that the idealized conditions used to derive equation (6) and the other equations that follow from it may not exist. The validity of this assumption for reverse faults as well as normal faults nonetheless remains a possibility, and is an objective for future research.

CONCLUSIONS

Some previous studies have suggested that tilting of beds adjacent to normal faults is caused by rigid-body rotation, others suggest that it involves distributed vertical simple shear. For rigid-body rotation, bed and fault tilting are identical, whereas for vertical shear bed tilting and fault tilting are related via equation (6); bed tilting will usually exceed fault tilting. For given non-zero present-day bed and fault dips θ and δ, these two assumptions predict different initial dips of normal faults δ_0 and different amounts of extension. Differences between bed and fault tilting for the two assumptions are greatest when the present-day fault dip δ equals the amount of bed tilting θ, which occurs when $\tan(\delta) = \tan(\delta_0)/2$.

We use observations of normal faults from western Turkey, the western United States, and the North Sea to distinguish between the two assumptions, given that δ_0 of about 45–65° is expected. For vertical shear, initial fault dips are within this range, but in many cases for rigid-body rotation they are not (Table 4). Other observations, including reversals of tilt polarity between closely-spaced normal faults (Fig. 5b), also support vertical shear. Vertical shear thus in general better

describes the deformation style in the surroundings of normal faults than rigid-body shear. Unlike rigid-body rotation, vertical shear is also consistent with realistic rheologies for, and expected stress fields in, the brittle upper crust.

This result has some important observational consequences. First, under vertical shear the heave of any normal fault equals the extension across it. Second, under vertical shear no feature can rotate through the vertical. A normal fault thus cannot rotate through the vertical and appear to be a reverse fault. Third, under vertical shear any feature that is initially vertical will remain vertical. A vertical dyke in the tilted surroundings of a normal fault is thus not necessarily younger than the extension that caused the tilting.

Acknowledgements—Supported in part by Natural Environment Research Council grants GR3/6966 and GR3/6967 (R. Westaway). We are particularly grateful to Alan Roberts and Graham Yielding for discussions that initiated and stimulated this investigation. We also thank Dan McKenzie, James Jackson, Nicky White and Celal Şengör for other helpful discussions, and Kay Lancaster for preparing the diagrams. Ron Bruhn and Dave Barr provided thoughtful and constructive reviews.

REFERENCES

Anderson, E. M. 1951. *The Dynamics of Faulting* (2nd edn). Oliver & Boyd, Edinburgh.

Axen, G. J. & Wernicke, B. P. 1989. Reply to comment by Carpenter, D. G., Carpenter, J. A., Bradley, M. D., Franz, U. A. & Reber, S. J. on "On the role of isostasy in the evolution of normal fault systems" by Wernicke, B. P. & Axen, G. J. *Geology* **17**, 775–776.

Axen, G. J. & Wernicke, B. P. 1991. Comment on "Tertiary extension and contraction of lower-plate rocks in the central Mojave metamorphic core complex, southern California" by Bartley, J. M., Fletcher, J. M. & Glazner, A. F. *Tectonics* **10**, 1084–1086.

Bartley, J. M., Fletcher, J. M. & Glazner, A. F. 1990. Tertiary extension and contraction of lower-plate rocks in the central Mojave metamorphic core complex, southern California. *Tectonics* **9**, 521–534.

Bruhn, R. L., Gibler, P. R. & Parry, W. T. 1987. Rupture characteristics of normal faults: an example from the Wasatch fault zone, Utah. In: *Continental Extensional Tectonics* (edited by Coward, M. P., Dewey, J. F. & Hancock, P. L.). *Spec. Publs geol. Soc. Lond.* **28**, 337–353.

Buck, R. W. 1988. Flexural rotation of normal faults. *Tectonics* **7**, 959–973.

Byerlee, J. 1978. Friction of rocks. *Pure & Appl. Geophys.* **116**, 615–626.

Carpenter, D. G., Carpenter, J. A., Bradley, M. D., Franz, U. A. & Reber, S. J. 1989. Comment on "On the role of isostasy in the evolution of normal fault systems" by Wernicke, B. P. & Axen, G. J. *Geology* **17**, 774–775.

Coney, P. J. & Harms, T. A. 1984. Cordilleran metamorphic core complexes: Cenozoic extensional relics of Mesozoic compression. *Geology* **12**, 550–554.

Emmons, W. H. & Garrey, G. H. 1910. General geology. In: *Geology and Ore Deposits of the Bullfrog District, Nevada* (edited by Ransome, F. L., Emmons, W. H. & Garrey, G. H.). *Bull. U.S. geol. Surv.* **407**, 19–89.

Hamilton, W. 1987. Crustal extension in the Basin and Range province, southwestern United States. In: *Continental Extensional Tectonics* (edited by Coward, M. P., Dewey, J. F. & Hancock, P. L.). *Spec. Publs geol. Soc. Lond.* **28**, 155–176.

Jackson, J. A. 1987. Active normal faulting and crustal extension. In: *Continental Extensional Tectonics* (edited by Coward, M. P., Dewey, J. F. & Hancock, P. L.). *Spec. Publs geol. Soc. Lond.* **28**, 3–17.

Jackson, J. A., King, G. C. P. & Vita-Finzi, C. 1982. The neotectonics of the Aegean: an alternative view. *Earth Planet Sci. Lett.* **61**, 303–318.

Jackson, J. A. & McKenzie, D. P. 1983. The geometrical evolution of normal fault systems. *J. Struct. Geol.* **5**, 471–482.

Jones, M. & Westaway, R. 1991. Microseismicity and structure of the Germencik area, western Turkey. *Geophys. J. Int.* **106**, 293–300.

King, G. C. P., Stein, R. S. & Rundle, J. B. 1988. The growth of geological structures by repeated earthquakes: 1. conceptual framework. *J. geophys. Res.* **93**, 13,307–13,318.

Kusznir, N. J., Marsden, G. & Egan, S. S. 1991. A flexural cantilever simple shear/pure shear model of continental lithosphere extension: applications to the Jeanne d'Arc basin, Grand Banks, and Viking graben, North Sea. In: *The Geometry of Normal Faults* (edited by Roberts, A. M., Yielding, G. & Freeman, B.). *Spec. Publs geol. Soc. Lond.* **56**, 41–60.

Marsden, G., Yielding, G., Roberts, A. M. & Kusznir, N. J. 1990. Application of a flexural cantilever simple shear/pure shear model of continental lithosphere extension to the formation of the northern North Sea basin. In: *Tectonic Evolution of the North Sea Rifts* (edited by Blundell, D. J. & Gibbs, A. D.). Oxford University Press, Oxford, 236–257.

Morton, W. H. & Black, R. 1975. Crustal attenuation in Afar. In *Afar Depression of Ethiopia* (edited by Pilger, A. & Rosler, A.). *Inter-Union Comm. Geodyn. Sci. Rep.* **14**, 55–65.

Parry, W. T. & Bruhn, R. L. 1987. Fluid inclusion evidence for a minimum 11 km vertical offset on the Wasatch fault. *Geology* **15**, 67–70.

Ramsay, J. G. 1967. *Folding and Fracturing of Rocks*. McGraw-Hill, New York.

Roberts, A. M. & Yielding, G. 1991. Deformation around basin-margin faults in the North Sea/mid-Norway rift. In: *The Geometry of Normal Faults* (edited by Roberts, A. M., Yielding, G. & Freeman, B.). *Spec. Publs geol. Soc. Lond.* **56**, 61–78.

Stein, R. S. & Barrientos, S. E. 1985. High-angle normal faulting in the Intermountain seismic belt: Geodetic investigation of the 1983 Borah Peak, Idaho, earthquake. *J. geophys. Res.* **90**, 11,355–11,366.

Stein, R. S., King, G. C. P. & Rundle, J. B. 1988. The growth of geological structures by repeated earthquakes: 2. field examples of continental dip-slip faults. *J. geophys. Res.* **93**, 13,319–13,331.

Turcotte, D. L. & Schubert, G. 1982. *Geodynamics: Applications of Continuum Physics to Geological Problems*. John Wiley, New York.

Verrall, P. 1981. Structural interpretation with application to North Sea problems. *Joint Ass. Petrol. Expl. Courses, course notes* 3.

Wernicke, B. P. & Axen, G. J. 1988. On the role of isostasy in the evolution of normal fault systems. *Geology* **16**, 848–851.

Westaway, R. 1990a. Block rotation in western Turkey: 1. observational evidence. *J. geophys. Res.* **95**, 19,857–19,884.

Westaway, R. 1990b. Seismicity and tectonic deformation rate in Soviet Armenia: implications for local earthquake hazard and evolution of adjacent regions. *Tectonics* **9**, 447–503.

Westaway, R. 1993. Neogene evolution of the Denizli region of western Turkey. *J. Struct. Geol.* **15**, 37–53.

Westaway, R., Gawthorpe, R. & Tozzi, M. 1989. Seismological and field observations of the 1984 Lazio–Abruzzo earthquakes: implications for the active tectonics of Italy. *Geophys. J.* **98**, 489–514.

Westaway, R. & Jackson, J. A. 1987. The earthquake of 1980 November 23 in Campania–Basilicata (southern Italy). *Geophys. J. R. astr. Soc.* **90**, 375–443.

White, N. J., Jackson, J. A. & McKenzie, D. P. 1986. The relationship between the geometry of normal faults and that of the sedimentary layers in their hanging walls. *J. Struct. Geol.* **8**, 879–909.

Yielding, G., Bradley, M. E. & Freeman, B. 1991. Seismic reflections from normal faults in the northern North Sea. In: *The Geometry of Normal Faults* (edited by Roberts, A. M., Yielding, G. & Freeman, B.). *Spec. Publs geol. Soc. Lond.* **56**, 79–89.

Ziegler, P. A. 1988. Evolution of the Arctic North Atlantic and western Tethys. *Mem. Am. Ass. Petrol. Geol.* **43**.